LOW TEMPERATURE TENSILE STRENGTH AND FRACTURE TOUGHNESS OF ASPHALT CONCRETE DETERMINED FROM SMALL NOTCHED 3-P-B SAMPLES

BINHUA WANG[†], OUMING XU[††], BIAO MA[†††], XIAOZHI HU[*†] AND PENGMIN LU[†]

[†]Chang'an University
Key Laboratory of Road Construction Technology and Equipment, MOE
Xi'an, 710064, PR China
e-mail: wangbh@chd.edu.cn

[† †]Chang'an University
School of Material Science and Engineering
Xi'an, 710061, PR China
e-mail: xuouming@yahoo.com

[† † †] Chang'an University
Key Laboratory of Ministry of Transportation Road Structure and Materials
Xi'an, 710064, China
e-mail: mabiaochd@163.com

[*] University of Western Australia
Department of Mechanical Engineering,
Perth, WA 6009, Australia
e-mail: xiao.zhi.hu@uwa.edu.au

Key words: Boundary effect model (BEM); Three-point-bend (3-p-b) test; Tensile strength; Fracture Toughness; Asphalt Concrete

Abstract: Cracking in asphalt concrete at low temperatures and relevant brittleness and toughness properties are primary concerns, considering the long-term complex road service conditions and economic impacts due to costly maintenance. In this study, we examine a simple closed-form solution for tensile strength f_t and fracture toughness K_{IC} measurements as the key cracking property characteristics of asphalt concrete. Although the limited size or thickness of real asphalt concrete structures invalidates the application of LEFM and fracture toughness K_{IC} criterion, a Boundary Effect Model (BEM) for quasi-brittle fracture of heterogeneous solids considering the combined effects of f_t and K_{IC} [11-13] overcomes the problem. Asphalt concrete AC-13 is chosen in this study, small notched three-point-bending (3-p-b) samples are tested at -10°C. The 3-p-b samples have width (or size) W = 35 mm, span S = 88 mm, and thickness B = 30 mm. Two different notch lengths of 7 and 10 mm (or α-ratio = a_0/W = 0.2 and 0.3) are selected for Group A and B samples to induce different notch and sample boundary interactions. The average aggregate size (or grain size) G of the asphalt concrete is around 5 mm, i.e. the a_0/G ratio is only between 1.4 and 2, making the samples highly heterogeneous. BEM analyses of test results show the relative error between the two groups for strength and toughness is less than 13%. If all tests are grouped together, the relative errors of Group A and B in comparison to the strength (f_t = 7.23 MPa) and toughness (K_{IC} = 1.81 MPa$\sqrt{m}$) of the total sample population are halved to 6%. These preliminary results show that the simple closed-form solution potentially can provide a reliable method for determination of low temperature fracture properties of asphalt concrete for optimization of materials mix for higher cracking resistance.

1 INTRODUCTION

Short surface cracking in quasi-brittle or elastic-plastic asphalt concrete pavements can post major problems for their service lifetime due to the stress concentration at cracking sites and invasion of micro-dust, which eliminates any chance of crack-healing [1,2]. The fracture toughness K_{IC} of a brittle homogeneous material as defined by Linear Elastic Fracture Mechanics (LEFM) is the key material property for cracking initiation and propagation, and is known to be an important material parameter of asphalt concrete [3,4]. However, direct application of K_{IC} for fracture analysis of asphalt concrete pavements is not possible as LEFM is invalid for such heterogeneous structures.

However, the significance of fracture properties of asphalt concrete has attracted increasing attention among researchers around the world [5,6]. In those studies, most of the mode I fracture toughness of asphalt concretes are tested in the shape of disc or beam samples subjected to three or four-point-bending, compression or tension loading, such as single edge notched beam (SENB) sample [7], edge cracked semi-circular bend (SCB) sample [6], edge-notched disc bend (ENDB) sample [8] and disc shape compact tension (DCT) sample [9]. However, how to reduce the influence of sample size on the fracture energy has always been the focus of research [10]. Yet, those aforementioned studies were carried out without appropriate theoretical models that explicitly consider the highly heterogeneous material structures of asphalt concrete.

In this study, we adopt a new simplified Boundary Effect Model (BEM) [11-13] to study the cracking properties of asphalt concrete because the model has explicitly included the aggregate measurement in its closed-form solution. The model is particularly useful to deal with short surface cracks in small samples or structures, e.g. with limited thickness such as asphalt concrete pavements. Here, boundary effect simply means interactions between a short surface crack and the free surface boundary.

Asphalt concrete AC-13 [14] with the average aggregate size G around 5 mm was selected and tested in this study. Notched three-point-bending (3-p-b) samples were tested at -10°C. Shallow surface notches (a_0) of 7 and 10 mm were introduced to simulate short surface cracks and study their influence on K_{IC} measurement. Note that the a_0/G is only around 2 or less, and normally K_{IC} cannot be determined in such case. BEM considering the combined effects of tensile strength f_t and fracture toughness K_{IC} is able to deduce K_{IC} measurements from quasi-brittle fracture events. It is found that consistent K_{IC} measurements have been obtained from small notched samples (width or size W = 35 mm, or W/G = 7) with two different notch depths (a_0 = 7 and 10 mm, or a_0/G = 1.4 and 2).

2. MAJOR BEM EQUATIONS FOR STRENGTH AND TOUGHNESS

The derivation details of BEM can be found in [11-13]. Here, we only give a brief introduction of its background and major equations for evaluation of the tensile strength f_t and fracture toughness K_{IC} of asphalt concrete.

One important feature of BEM is that the highly heterogeneous composite structures of asphalt concrete has been considered in modelling. Under the monotonically increased load, any zig-zag quasi-brittle crack growth or the fictitious crack growth Δa_{fic} at the notch tip a_0 is assumed to take place in a stepwise manner around aggregates. Because of the highly heterogeneous aggregate structures around the notch tip, Δa_{fic} varies from specimen to specimen as shown in Fig. 1(a) and (b). Therefore, a discrete number β (e.g. = 0.5, 1.0, 1.5 …) is introduced to consider the variation in Δa_{fic}, i.e.

$$\Delta a_{fic} = \beta \cdot G \tag{1}$$

As illustrated in Fig. 1, a group of seemly identical specimens will have different fracture

load P_{max} values due the variation in Δa_{fic}. It is assumed that the discrete number β follows the normal distribution.

Consider a group of 3-p-b samples (i =1, 2, 3, …), the fracture load $P_{\max-i}$ will be affected by Δa_{fic-i}, as shown in Fig. 1 (a). The concept of β-normal distribution illustrated in Fig. 1(c) was adopted [12]. The normal distribution is then used to analyze the tensile strength f_t from 3-p-b sample tests of any size and geometry.

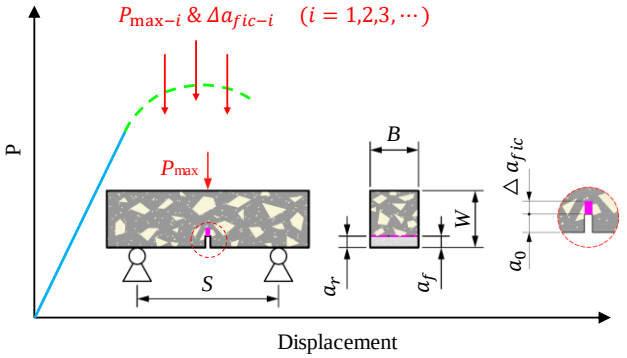

(a) Vertical displacement at loading point

(b) Notch tip details of 3-p-b sample

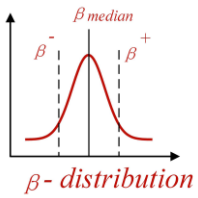

(c)

Figure 1: 3-p-b sample. Dimensions are as follows: W=35mm, S=87.5mm, B=30mm and a_0=7 &10mm.

$$P_{\max} = f_t \cdot A_e(W, a_0, G) = f_t \cdot \frac{W^2(1-\alpha)\cdot\left(1-\alpha+\frac{3\cdot G}{W}\right)}{1.5\cdot(S/B)\cdot\sqrt{1+\frac{a_e}{3\cdot G}}} \quad (2)$$

As shown in [15], Eq. (2) is obtained after substituting Eq. (1) and another discrete consideration of the characteristic crack into the final BEM in [11,12]. Where a_e is the equivalent crack [13]. It is assumed that the variation in the tensile strength f_t will also follow the normal distribution similar to the discrete number β.

For every $P_{\max}$ measurement, a f_t estimation is obtained. Consider a group of test samples, i.e. i = 1, 2, 3, …, it can be written from Eq. (2) that:

$$f_{t-i} = P_{\max-i} \cdot \frac{1.5\cdot(S/B)\cdot\sqrt{1+\frac{a_e}{3\cdot G}}}{W^2(1-\alpha)\cdot\left(1-\alpha+\frac{3G}{W}\right)} \quad (i=1,2,3,\cdots) \quad (3)$$

$$f_{t-i} = \frac{1}{\sqrt{2\pi}\sigma} e^{-\frac{[f_{t-i}-\mu]^2}{2\sigma^2}} \quad (i=1,2,3,\cdots) \quad (4)$$

Where μ and σ are mean value and standard deviation in f_t values. Then, the f_t in Eq. (2) can be replaced by $\mu \pm 2\sigma$ so that the mean straight line and scatter band with 95% reliability can be predicted as shown in Eq. (5). It is most convenient to present results in the linear relation between P_{max} and A_e (equivalent area).

$$P_{\max} = (\mu \pm 2\sigma)\cdot A_e(W, a_0, G) = (\mu \pm 2\sigma)\cdot \frac{W^2(1-\alpha)\cdot\left(1-\alpha+\frac{3\cdot G}{W}\right)}{1.5\cdot(S/B)\cdot\sqrt{1+\frac{a_e}{3\cdot G}}} \quad (5)$$

3. MATERIALS AND NOTCHED 3-P-B SAMPLE DIMENSION

The aggregate gradations and their percentages of asphalt mixtures in this study have been presented in Tab. 1. In order to manufacture the 3-p-b sample from AC-13 asphalt mixtures, first square sample was prepared using compactor. It was then sliced into several beams with dimensions of 125×35×30 mm^3 by means of a masonry sawing machine. Pre-crack was then generated

in the middle of 3-p-b samples utilizing a dry cutting machine with a 1.8 mm thickness blade. Fig.1 (a) and (b) show the dimensions and loading conditions of the small notched 3-p-b samples of asphalt mixture. The samples have W = 35 mm, S/W = 2.5, and two different notch lengths of a_0 =7 mm and a_0 =10 mm, or α -ratios (= notch/W) of 0.2 and 0.3. It should be noted that when calculating the pre-notch length of each sample, considering the processing deviation of prefabricated notches, the average value $\frac{a_f + a_r}{2}$ of the front notch depth a_f and rear notch depth a_r are determined to a_0. The detailed dimensions of all samples including group A and group B were shown in Tab. 2 and Tab. 3.

Table 1: Gradation of A-13 asphalt binder

Gradation /mm		AC-13
Percentage passing through different sieve sizes (%)	16	100
	13.2	95
	9.5	76
	4.75	46
	2.36	32
	1.18	20
	0.6	16
	0.3	11
	0.15	9
	0.075	6

Table 2: Detailed dimensions of sample in Group A

Group A				
No	a_0 /mm	B /mm	W /mm	S /mm
1	7.16	30.00	33.80	87.5
2	6.93	30.52	35.46	87.5
3	7.08	29.95	33.67	87.5
4	7.10	30.83	35.13	87.5
5	6.67	30.42	35.09	87.5
6	6.61	30.20	35.04	87.5
7	6.96	30.21	35.92	87.5
8	6.77	30.06	35.32	87.5
9	6.93	29.78	35.02	87.5
10	7.10	30.35	33.47	87.5
11	7.05	30.86	35.57	87.5
12	6.92	30.79	35.61	87.5
13	7.02	29.95	34.28	87.5
14	7.06	30.74	35.16	87.5
15	6.70	30.51	35.01	87.5

Table 3: Detailed dimensions of sample in Group B

Group B				
No	a_0 /mm	B /mm	W /mm	S /mm
1	10.48	30.20	35.82	87.5
2	10.30	30.57	34.73	87.5
3	9.89	29.78	34.88	87.5
4	9.90	30.53	34.69	87.5
5	9.80	30.79	34.01	87.5
6	10.35	30.03	35.06	87.5
7	10.34	29.84	35.11	87.5
8	10.13	30.56	34.67	87.5
9	9.63	30.80	36.09	87.5
10	10.31	29.24	34.45	87.5
11	10.07	30.56	35.09	87.5
12	10.28	29.69	36.18	87.5
13	10.04	30.55	33.96	87.5
14	10.39	30.38	34.60	87.5
15	10.11	30.34	34.96	87.5

4. 3-P-B EXPERIMENTS

Figure 2: 3-p-b testing system. Temperature was controlled at -10℃ and displacement rate of cross-head was kept at 1mm/min.

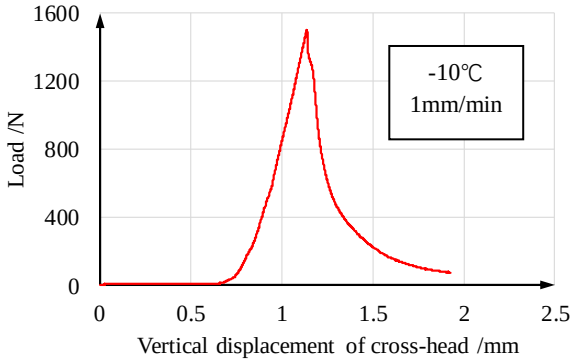

Figure 3: Typical load-displacement curves of pre-notched samples at the 3-p-b testing.

The 3-p-b tests were conducted at temperature -10℃. The pre-notched samples were first placed in freezer at -10℃ for 3 hours to ensure all parts of samples at the same temperature. The compression tests were carried out directly in freezer using universal testing machine and a three-point bend fixture, as shown in Fig. 2. The cross-head was loaded at a speed of 1mm/min under displacement control mode, and stopped when load drops to 10% of the maximum load.

Tables 4: Tensile strength and fracture toughness results of notched 3-p-b samples with notch/W ratios = 0.2 and 0.3.

Group	No	P_{max} /N	G=5.2 mm	
			f_t /MPa	K_{IC} /MPa√m
A	1	1631.70	7.15	1.79
	2	1499.98	5.77	1.44
	3	1429.15	6.29	1.57
	4	1543.24	6.06	1.51
	5	1652.54	6.41	1.60
	6	1742.28	6.79	1.70
	7	2103.51	7.99	2.00
	8	1723.70	6.72	1.68
	9	2284.92	9.25	2.31
	10	1482.35	6.53	1.63
	11	1495.50	5.71	1.43
	12	1578.50	5.97	1.49
	13	1631.06	6.89	1.72
	14	1559.28	6.12	1.53
	15	2115.68	8.23	2.06
B	1	1324.98	6.46	1.61
	2	1461.52	7.44	1.86
	3	1587.47	7.98	1.99
	4	1408.32	6.99	1.75
	5	1729.80	8.83	2.21
	6	1392.30	7.09	1.77
	7	1314.73	6.71	1.68
	8	1666.32	8.42	2.10
	9	1582.99	7.00	1.75
	10	1309.27	7.10	1.77
	11	1811.19	8.86	2.21
	12	1924.66	9.20	2.30
	13	1615.05	8.49	2.12
	14	1443.25	7.51	1.88
	15	1379.46	6.88	1.72

As shown in Fig. 3, the curves of load versus displacement of cross-head were recorded from fracture tests at the temperature -10℃. It can be seen that the curves present a better linear shape before the peak load resulting from the obvious brittle fracture behavior of asphalt concrete beam. The details of test result are shown in Tab. 4, also the relation between f_t and K_{IC} through grain size parameter of G is calculated as [13]

$$K_{IC}=2\cdot f_t\cdot\sqrt{3\cdot G} \tag{6}$$

The tensile strength f_t and the fracture toughness K_{IC} were calculated by using Eq. (3) and Eq. (6) shown in Tab.4, respectively.

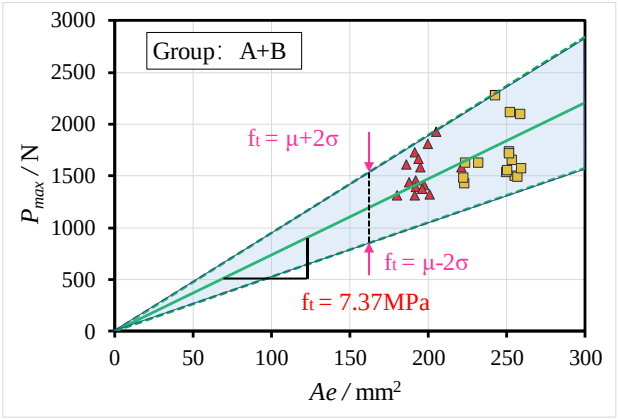

(a)

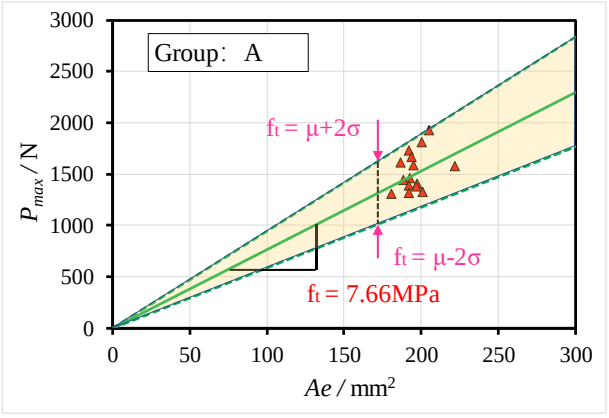

(b)

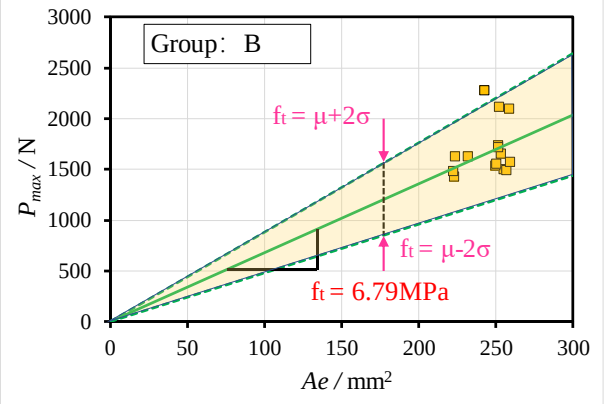

(c)

Figure 5: Prediction of tensile strength f_t using curve fitting and normal distribution analysis based on all P_{max} data .

The mean and reliability lines of the tensile strength f_t according Eq. (4) were expressed by green solid and blue dotted lines drawn in Fig. 5. And it can be seen clearly from Fig. 5 that the dispersed test results can be covered almost between the upper and lower bounds with 95% reliability for all samples, Group A or Group B. The average tensile strength and fracture toughness of group A and group B are only 6% relative error to all samples, as illustrated in Tab. 5.

Table 5: Average values of f_t and K_{IC} for Group A, Group B and Group (A+B)

Group	Average of f_t /MPa	Average of K_{IC} /MPa√m	Relative error
A+B	7.23	1.81	0
A	6.79	1.70	-6%
B	7.66	1.91	6%

4. DISCUSSIONS

The simplified BEM shows that the linear relation between fracture load P_{max} and equivelant area A_e has the tensile strength f_t as its slope. This makes BEM easy to use, and its data analysis simple to perform. Furthermore, the linear BEM goes through the origin (0,0), i.e. in principle only one more point needs to be measured to fully determine the linear relation. This is exactly the case if group A and B are considered separately (or only group A or B tests were performed). The two "one-pont" f_t measurements are 6.79 and 7.66 MPa, and the relative error between them is less than 13%. Experimental errors of such a magnitute are acceptable, considering the asphalt concrete samples used in this study are highly heterogeneous and only 15 samples were tested for each group. Considering the *W/G* ratio is only 6 and the a_0/G ratio is only between 1.4 and 2, the relative error of 6% between the combined A+B and group A or B is almost perfect.

Another useful feature of the linear BEM is that the statistical scatters in experiments can be easiy analysed and predicted with a specified reliability, e.g. 95%. If two asphalt concrete materials have the same strength and toughness values (but different standard deviations), one can draw the conclusion from the BEM analysis that cracking may first appear in the asphalt concrete mix with higher standard deviation. Certainly the design applications of BEM warrant further investigation.

5. CONCLUSIONS

Highly heterogeneous asphalt concrete samples with two different notch lengths, a_0 = 7 and 10 mm, have been tested under 3-p-b conditions, and analyzed using a simple closed-form solution evolved from the boundary effect model (BEM). The *W/G* ratio is only 6 (sample-size over grain-size = 30/5), but the a_0/G ratio is even smaller, between 1.4 and 2. Yet, both the tensile strength f_t and fracture toughness K_{IC} of the asphalt concrete have been determined. f_t = 7.23 MPa determined from the present study under the displacement rate of 1 mm/min appears to be supported by separate strength measurements, f_t = 8.68 MPa, under much higher displacement rate of 50 mm/min at -10°C.

It is encouraging to see that even the two groups of tests are considered separately, the relative error between their strength estimatios is still less than 13%.

Although the fracture toughness K_{IC} cannot be used directly to determine fracture of asphalt directly (it is not the case of LEFM),

its value potentially is still useful in characterization of the low temperature cracking behaviour of asphalt concrete. It is possible that K_{IC} together with the specific fracture energy GF [10,16] can be utilized in optimization of asphalt concrete material compositions and properties against asphalt cracking in low temparature enviornments.

REFERENCES

[1] Fan, S., Wang, H., Zhu, H. and Sun, W., 2018. Evaluation of Self-Healing Performance of Asphalt Concrete for Low-Temperature Fracture Using Semicircular Bending Test. *J. Mater. Civ. Eng.* **30**(9): 04018218.

[2] Riara, M., Tang, P., Mo, L., Jacilla, B. and Wu, S., 2018. Investigation into crack healing of asphalt mixtures using healing agents. *Constr. Build. Mater*. **161**: 45-52.

[3] Sun, L., Ren, J., Zhang, S., 2018. Fracture Characteristics of Asphalt Concrete in Mixed-Loading Mode at Low-Temperature Based on Discrete-Element Method. *J. Mater. Civ. Eng.* **30**(12): 04018321.

[4] Aliha, M.R.M., Shaker, S. and Keymanesh, M. R., 2019. Low temperature fracture toughness study for bitumen under mixed mode I+ II loading condition. *Eng. Fract. Mec*h. **206**: 297-309.

[5] Wagoner, M.P, Buttlar, W.G. and Paulino, G.H., 2005. Development of a single-edge notched beam test for asphalt concrete mixtures. *J. Test. Eval.* **33**(6): 452-460.

[6] Im, S., Kim, Y.R and Ban, H., 2013. Rate- and temperature-dependent fracture characteristics of asphaltic paving mixtures. *J. Test. Eval.* **41**(2): 257-268.

[7] John, R., Shah, S.P., 1990. Mixed-mode fracture of concrete subjected to impact loading. *J. Struct. Eng*. **116**(3): 585-602.

[8] Pour, P.J.H., Aliha, M.R.M. and Keymanesh, M.R., 2018. Evaluating mode I fracture resistance in asphalt mixtures using edge notched disc bend ENDB specimen with different geometrical and environmental conditions. *Eng. Fract. Mech*. **190**: 245-258.

[9] Stewart, C.M., Oputa, C.W. and Garcia, E., 2018. Effect of specimen thickness on the fracture resistance of hot mix asphalt in the disk-shaped compact tension (DCT) configuration. *Constr. Build. Mater*. **160**: 487-496.

[10] Wagoner, M.P., Buttlar, W.G., 2007. Influence of specimen size on fracture energy of asphalt concrete (with Discussion). *J. Assoc. Asphalt Paving Technol.* **76**.

[11] Wang, Y.S., Hu, X.Z., Liang, L. and Zhu, W.C., 2016. Determination of tensile strength and fracture toughness of concrete using notched 3-p-b specimens. *Eng Fract Mech.* **160**: 67–77.

[12] Hu, X.Z., Guan, J.F., Wang, Y.S., Keating, A. and Yang, S.T., 2017. Comparison of boundary and size effect models based on new developments. *Eng Fract Mech.* **175**: 146–167.

[13] Guan, J.F., Yuan, P., Hu, X.Z., Qing, L. and Yao, X., 2019. Statistical analysis of concrete fracture using normal distribution pertinent to maximum aggregate size. *Theor. Appl. Fract. Mech.*

[14] Research Institute of Highway Ministry of Transportation., 2004. Technical specifications for construction of highway asphalt pavements (JTG F40-2004). Beijing: China Communica-tions Press. (In Chinese).

[15] Chen, Y., Han C.Y., Hu, X.Z., Wang, B.H., Zhu, W.C., 2019. Strength criterion for size effect on quasi-brittle fracture with and without notch. In Proceedings of FraMCoS-X, France, June 24-26, 2019.

[16] Hu, X.Z., Wittmann, F.,1992. Fracture energy and fracture process zone. *Mater.*

Struct. **25**, 319-326.